Sensors & Actuators: B. Chemical 422 (2025) 136662

Contents lists available at ScienceDirect

Sensors and Actuators: B. Chemical

journal homepage: www.elsevier.com/locate/snb

Novel usage of perinone polymer as solid contact in ion-selective electrodes

Klaudia Morawska [a], Malgorzata Czichy [b,c], Patryk Janasik [b], Mieczyslaw Lapkowski [b,c,d], Cecylia Wardak [a,*]

[a] Department of Analytical Chemistry, Institute of Chemical Sciences, Faculty of Chemistry, Maria Curie-Sklodowska University, Maria Curie-Sklodowska Sq. 3, Lublin 20-031, Poland
[b] Faculty of Chemistry, Silesian University of Technology, M. Strzody 9, Gliwice 44-100, Poland
[c] Centre for Organic and Nanohybrid Electronics, Silesian University of Technology, Konarskiego 22b, Gliwice 44-100, Poland
[d] Centre of Polymer and Carbon Materials, Polish Academy of Sciences, Curie-Sklodowska Str. 34, Zabrze 41-819, Poland

ARTICLE INFO

Keywords:
Perinone polymers
Solid contact
Ion-selective electrode
Multiredox conducting polymers
Potentiometry

ABSTRACT

The paper presents the use of a new perinone polymer (PPer) as an intermediate layer and the development of a new type of potassium ion-selective electrodes with solid contact. The PPer layer was applied to the surface of a glassy carbon electrode using potentiodynamic polymerization from an electrolyte solution containing perinone precursors (Per). Subsequently, the surface of the electrode after application of the polymer was examined using a microscope and an optical profilometer. To check the quality of the prepared ion-selective electrodes, a series of tests were carried out and the analytical and electrical parameters of the electrodes were determined. Electrode modifications using PPer improved the electrode parameters, especially the stability and reversibility of the potential, compared to the control electrode covered only with an ion-sensitive membrane. The best electrode was the electrode modified with PPer applied in 10 cycles, which, as a result of the modification, allowed better parameters to be obtained – slope 58.86 mV/decade, LOD 1.2×10^{-6} M, linearity range $5 \times 10^{-6} - 1 \times 10^{-1}$ M. A very low short-term potential drift value of 2.7×10^{-4} mV/s was obtained as well as an extremely satisfactory SD value of 1.1 mV from E^0 measurements. The modification also improved electrical properties and gave a negative result of the water layer test.

1. Introduction

Ion-selective electrodes with solid contact (SCISEs) are currently the most intensively researched group of electrodes. There is no internal electrolyte solution in these electrodes, so an additional layer called a solid contact is used here between the membrane and the substrate [1]. A solid contact is a material that provides good ion-to-electron conductivity and is characterized by chemical stability and inertness, hydrophobicity, high electrical capacitance, and mechanical resistance. A well-chosen solid contact ensures adequate ion-to-electron conductivity between the membrane and the electrode substrate, which contributes, among other things, to improved potential stability [2–5]. When selecting a solid contact, we must also remember that it must be compatible with the components of ion-selective membranes (ISMs) to enable its use in sensors for versatile ion detection, which is why its inertness is also important[6,7]. Among the most popular solid contact materials are conductive polymers[8–10], carbon nanomaterials [11–13], metal nanoparticles and metal oxides[14–16], as well as hybrid[17,18] and composite materials[19–21].

Various conductive materials can be used as a solid contact, but different properties of such materials should be taken into account. Thus, the electrical conductivity of polymers may be different depending on the type of charge carriers (free valence electrons, excess electrons, holes, ions) and may also be mixed. In addition to the chemical structural features, conductivity is also influenced by external factors such as temperature, electric and magnetic fields, electromagnetic radiation, chemical environment, the presence of non-specific interactions affecting the macroscopic ordering, etc. Π-electrons of conjugated systems are responsible for the conductivity in the neutral state, especially in regioregular linear systems[22–25] as well as in systems with limited rotation between monomer subunits, e.g. ladder polymers such as poly (benzimidazobenzophenanthroline) (BBL)[26–31]. Limited rotation of meric subunits can also be achieved by obtaining a quinoid structure after oxidation or reduction of the π-conjugated systems, where the conductivity is associated with the migration of polaronic or bipolar states (doped states). These positive or negative polarons/bipolarons

* Corresponding author.
E-mail address: cecylia.wardak@mail.umcs.pl (C. Wardak).

https://doi.org/10.1016/j.snb.2024.136662
Received 16 July 2024; Received in revised form 13 September 2024; Accepted 18 September 2024
Available online 19 September 2024

also exist due to the presence of appropriate counter ions that compensate for the charges of the macromolecules[32]. Not only intramolecular transfer but also intermolecular one is responsible for charge transfer, which is particularly important in donor-acceptor polymers. The presence of specific donor-acceptor structural motifs can create charge transfer (CT) complexes responsible for the conductivity of such material, especially under the influence of thermal or light energy, etc.[33]. Intermolecular conductivity may also occur as a result of the reversible electron transfer between stable redox centers of the polymer, taking place in the environment of an ionic conductor. Typical ionic conductivity occurs in ionomers, resulting from the dissociation of a proton or other ion into the environment and its transfer in an electric field[34].

The properties of conductive polymers can be modified for specific applications. When used as interlayers in ISEs, hydrophobicity is important. This parameter can also be significantly improved by introducing highly hydrophobic ions into the polymer structure[35]. Increased hydrophobicity and efficiency in charge transfer can also be achieved by combining a conductive polymer with other materials to form copolymers, composites or hybrid materials[36–38]. In each case, however, this requires additional operations, so the search continues for conductive polymers that can act effectively as a solid contact and are relatively simple to produce.

Taking into account contemporary knowledge about conductive polymers and the expectations placed on the solid contact in ion-selective sensors, a new perinone polymer was proposed for several reasons. Firstly, due to its structural features, this polymer has a very good structural affinity both for the electrode material, i.e. glassy carbon (GC) (aromatic segments and partially ladderization) and also to ion-sensitive membrane (stable redox centers with trapped ions), and all this in one polymeric structure (without the need to use a composite) in an easy, cheap and ecological electropolymerization process[24,25]. Additionally, this polymer exhibits many reversible redox states in a very wide potential window. Secondly, perinone monomers can also be obtained in a simple condensation reaction, like many known perinone dyes (containing an amide-amidine system) (Fig. 1)[22,39–48]. The monomer precursors are usually aromatic (di)anhydrides and a suitable diamine. In our case, 1,8-naphthalenamine was used, which leads to the formation of a perimidine unit in the monomer structure, through which new bonds were formed giving perinone polymers[49–52]. This paper presents the first use of perinone polymers (PPer) in the construction of potassium solid contact ion-selective electrodes, whose design was enriched with an intermediate layer constituted by a PPer deposited by electropolymerization from Per solution (Figs. 1, a-1).

2. Materials and methods

2.1. Materials and measurements as seen in supporting information

.

2.2. Preparation of ion-selective electrodes

2.2.1. Preparation of PPer intermediate layer

Before applying the intermediate layer, the surface of the GCE was properly pre-prepared[53]. A perinone polymer was deposited from a

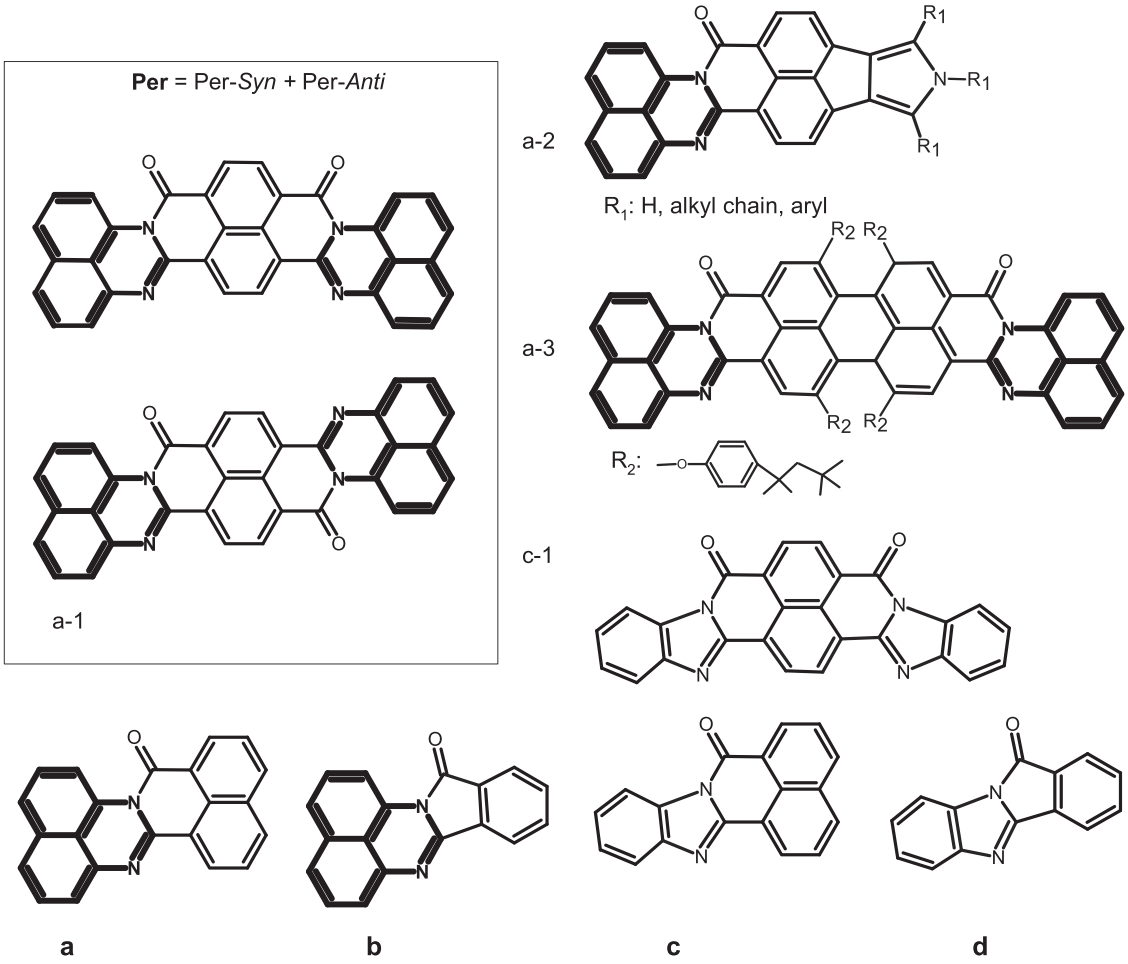

Fig. 1. Examples of perinones (a-d) also containing the perimidine segment (a, b); mixture of perinone isomers (a-1 = Per) as the system subjected to electropolymerization in the discussed work.

saturated Per solution obtained as a result of dissolving 0.2 mg of Per in 2 mL of 0.1 M solution of tetrabutylammonium hexafluorophosphate in dichloromethane. To carry out electropolymerization (potentiodynamic), software was run to set the parameters of the procedure carried out in cyclic voltammetry mode (in the positive potential range from −0.4–1.00 V vs. Fc/Fc^+ redox couple as the external reference; 50 mV/s). The stabilization process was conducted under the same conditions and parameters as the polymerization process. The difference was that for each electrode the stabilization was carried out in 5 cycles and the electrolyte solution did not contain Per monomers.

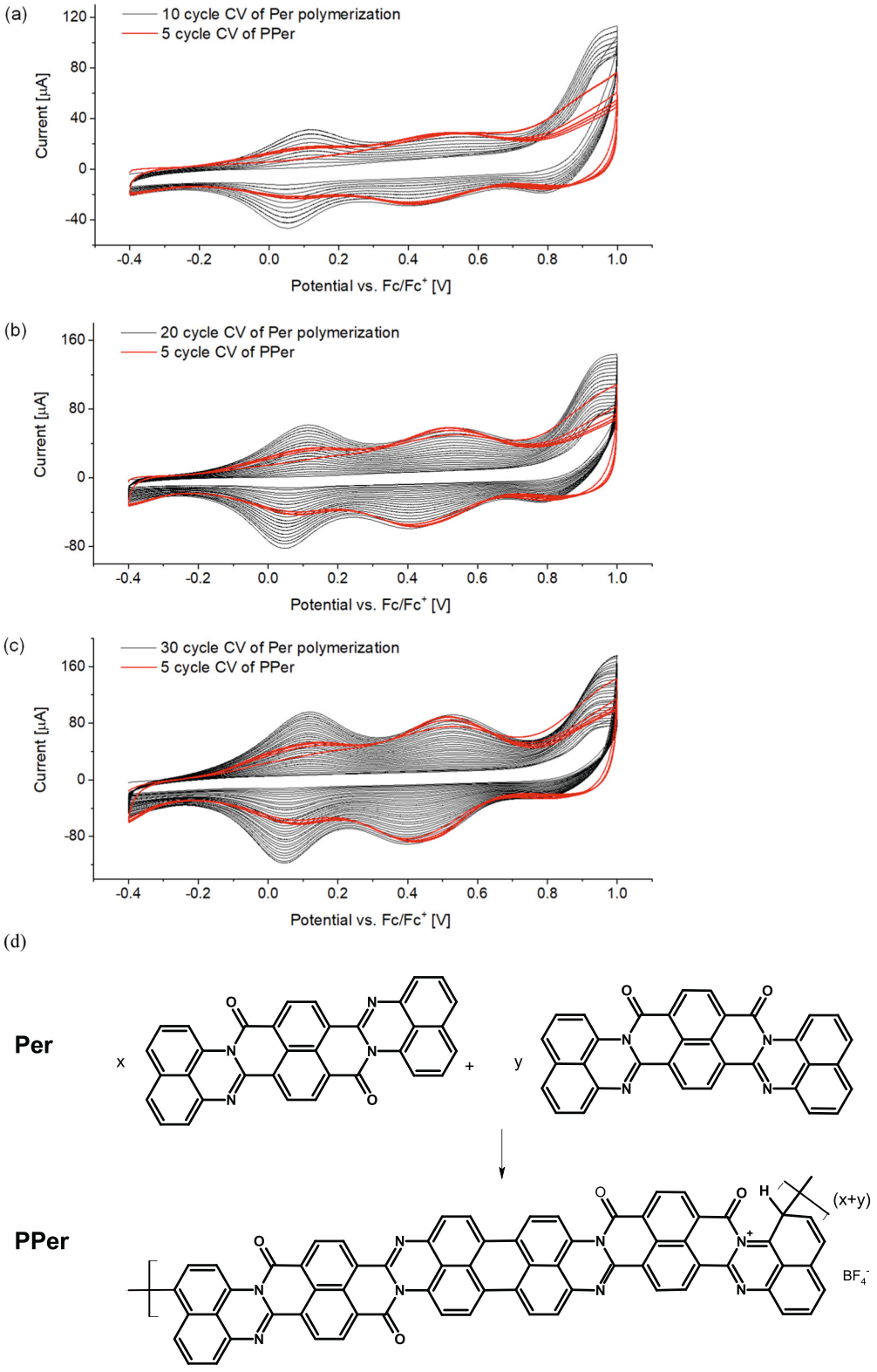

Fig. 2. The CV curves of electropolymerization of Per and their stability; the PPer polymers deposited under 10 (a), 20 (b), and 30 CV cycles (c) as solid contacts for GCEs; electropolymerization of Per and the PPer structure obtained in the range of −0.4–1.0 V and after stopping at −0.4 V (vs Fc/Fc^+) (d).

2.2.2. Preparation of ion-sensitive membrane and application to the electrode substrate

The next step was the application of an ion-selective membrane. For this purpose, a membrane cocktail with the following composition (wt./wt.): 64 % DOS, 32 % PVC, 3 % valinomycin and 1 % KTpClB, was applied to the surface of the inner electrode (3×50 µl). After solvent evaporation, the prepared electrodes were conditioned in 1×10^{-3} M KNO_3 solution for two days. Similarly, electrodes without the polymer interlayer were prepared. In this case, the membrane cocktail was drop-casted directly onto the cleaned unmodified GCE. Three electrodes of each type were made and tested in parallel.

3. Results and discussion

The purpose of the study was to test the possibility of using a new polymer from the perinone group as an intermediate layer in the design of ion-selective electrodes. This polymer had not been studied in this regard before. The subjects of the study were three types of electrodes differing in the thickness of the layer (the number of cycles in the application step) of the perinone polymer, which was the intermediate layer of the electrodes that were marked GCE/PPer-10c/K^+-ISM (10 cycles), GCE/PPer-20c/K^+-ISM (20 cycles), GCE/PPer-30c/K^+-ISM (30 cycles), respectively, and an unmodified electrode without the PPer layer (GCE/K^+-ISM).

3.1. Preparation of the intermediate layer of the GCE/PPer in the in situ electropolymerization of Per

PPer layers were deposited on the GCE by electropolymerization from a Per solution (Fig. 2a-c). Electropolymerization was carried out to obtain a specific structure of the PPer, as in Fig. 2d. The desirable state of the PPer was controlled in the process of potentiodynamic polymerization, which enabled the oxidation of the Per precursor (oxidation peak at 0.87 V) and then obtaining the appropriate oxidized state of PPer (the process stopped at −0.4 V vs. Fc/Fc^+). Each subsequent voltammetric cycle allowed for an increase in the amount of the deposited polymer. The electrodeposited PPer is a multi-redox polymer partially π-conjugated, with 3 redox states with the first one permanently charged: 0.1 V, 0.4 V and 0.9 V – from the protonated bis-perimidine unit (radical cation/dication), double-bonded deprotonated bis-perimidine and single-bonded deprotonated ones, respectively. The PPer cannot be completely discharged due to the strong hydrogen interaction of the hydrogen atom and the oxygen of the amino group, which was, however, a favorable state due to an ISM coating in the next stage. Full charging of the PPer was not used to ensure a longer life of the sensors and greater adhesion to the GCE. The thickness of the PPer interlayer was controlled using three different numbers of potential sweep cycles (10 – Fig. 2a, 20 – Fig. 2b, Fig. 2c – 30 CVs) and was further analyzed by comparing the effect of this parameter on the properties of the obtained GCE/PPer/ISM. The PPer layers obtained directly on the GCE during the in-situ electropolymerization made it possible to obtain coatings very well attached to the GCE electrodes, which is confirmed by the sweeping potential of the GCE-PPer in the range of −0.4–1.0 V in an electrolyte solution without Per, thus confirming again the presence of three typical and reversible redox states of this polymer. The current intensity remained at a similar level in subsequent cycles, which confirms the stability of the deposited PPer.

3.2. Examination of intermediate layer properties

The freshly applied PPer polymer layer is visible at the right angle to the naked eye. A series of further tests were conducted to verify the GCE surface coverage rate and the polymer layer's structure and morphology. An image of the GCE electrode taken before and after applying the perinone polymer using an optical microscope (Figure S2, a-d) showed that the PPer polymer film covers the entire surface area constituted by the glassy carbon, which proves that the method of polymer electrodeposition from solution is a good one for depositing these types of conductive polymers.

Extremely important is the specific surface area of the electrodes – as it grows, the electrical capacitance of the conductor increases, which depends, among other things, on its size. By obtaining a developed surface characterized by roughness and a significantly increased surface area, the amount of charge that can be received and then transferred at the same time is increased, which translates into more efficient charge transfer and therefore an improvement in electrical parameters of the layer. The study of the geometric structure of the polymer layer was carried out by optic profilometry. Based on the results, the averaged roughness (Ra) was determined. The Ra for the unmodified electrode was 27.3 nm. For the surface coated with the perinone polymer in 10 cycles, the roughness increased almost 20 times (Ra=489.14 nm), which indicates the increased irregularity of the surface and thus an enhanced specific surface area of the electrode substrate. Visually, we can see the transition of the uniform, flat surface, seen in Fig. 3a, into a heterogeneous surface, which has a rather elaborate structure forming a structure resembling a rock formation or mountainous terrain (Fig. 3b). In the case of the electrode, where the polymer film was applied at 20 cycles, we notice a smoothing of the surface, which is most likely due to the polymer chain entering deep into the highly heterogeneous surface (Fig. 3c). The result is a less rough surface, where the Ra parameter is 71.5 nm. Applying the polymer to such a surface for 10 subsequent cycles, we again observe the formation of an irregular layer and a significant increase in the specific surface area. Therefore, in the electrodes where the intermediate layer was applied in 30 cycles, we observed meanders and hills (Fig. 3d) that contributed to an increase in roughness, which was 215.39 nm for this electrode.

The reasons for the changes in roughness over successive deposition cycles are the mechanism of nucleation and the growth of the PPer. This process is multiple and multi-stage and the final roughness of the PPer interfacial layer may depend on the number of voltammogram cycles. However, the polymer roughness does not always have to decrease with the number of cycles for several reasons. Firstly, the nucleation process depends on many factors – the quality of the electrode material, monomer concentration, diffusion, distribution of electric field forces on a clean electrode and on an electrode partially or completely coated with polymer, etc. Secondly, these parameters will be different and these may have different effects on the three key process stages – the formation of the first polymer grains with lots of pores (up to a. 10 cycles), obtaining an almost complete coverage of the electrode and a relatively smooth polymeric surface (up to a. 20 cycles), and again uneven polymer growth (up to a. 30 cycles), etc. Obviously, the division of nucleation phases within voltammetric cycles may vary depending on the system and conditions. Here, until the 10th cycle, we observe the first stage of rapid PPer nucleation, because the monomer concentration at the electrode itself is then the highest. As the process progresses, the monomer concentration at the electrode itself decreases and remains constant deep in the solution (slower monomer diffusion than the process itself). We did not use stirring of the solution to continuously supply the monomer to the electrode surface due to inefficiency and less control over the growth of the polymer itself. Additionally, areas containing GCE crystal defects are preferred for the initial nucleation. Therefore, the first stage of electropolymerization ensures obtaining the highest significant roughness of the PPer. The second stage (up to cycle 20) is the process of further covering the electrode with the polymer until it is completely covered. An even layer is obtained at this stage due to the presence of the monomer trapped in the pores of the PPer, which undergoes electropolymerization (its concentration in the pores may be higher than on the polymer surface). However, it should be clearly indicated that this polymer layer also contains surface defects that cause uneven further polymer growth in the next stage. Thus, under the indicated conditions, this process can be divided into alternating electropolymerization on the "hills" or in the pores of the PPer. It is therefore important to control this

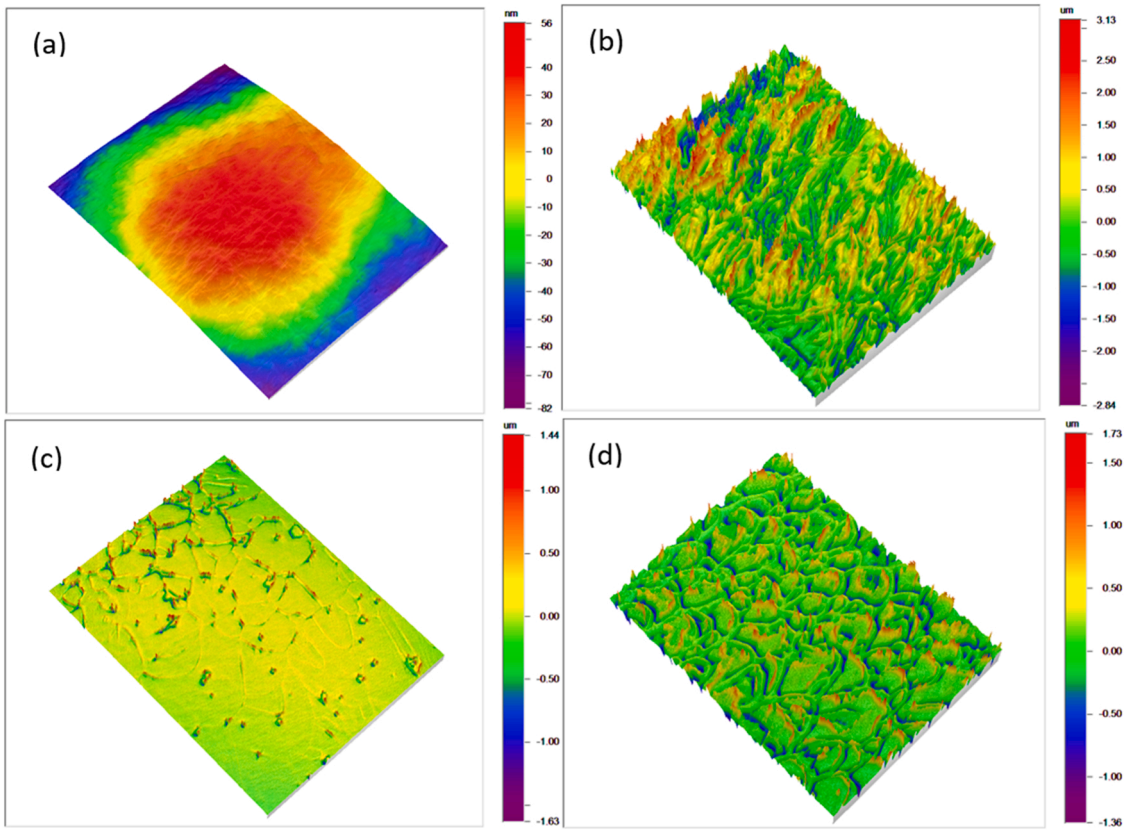

Fig. 3. The geometric structure of the PPer layers determined by optic profilometry - unmodified GCE surface (a), GCE/PPer-10c (b), GCE/PPer-20c (c), and GCE/PPer-30c (d).

growth and stop it at the right stage. Upon deposition onto the GC plate, the PPer exhibited a thickness of 10 nm after undergoing 10 cycles of deposition. The next cycles of deposition resulted in a gradual increase in thickness and for 30 cycles of deposition we obtained a layer with a thickness of around 50 nm. The layer thickness depends linearly on the number of deposition cycles (Fig. S3, f).

3.3. Potentiometric response

To determine the characteristics of each electrode, calibration was performed in a solution of K^+ ions (KNO_3 solution), in the concentration range of $1 \times 10^{-1} - 1 \times 10^{-7}$ M from the lowest to the highest concentration. The measurements were repeated weekly over three months. An example of one calibration curve from each month is shown in Fig. 4. Based on the curves, the basic analytical parameters determined for each electrode are shown in Table 1. All of the electrodes showed a very good slope close to Nernst values, but it was the GCE/10c_PPer/ISM electrode that exhibited the highest sensitivity of 58.86 mV/dec, which remained stable during the three months. The presence of the PPer as well as the layer thickness did not significantly affect the detection limit – the LOD for each electrode remained at the micromolar determination value throughout the measurement period. Similarly, for the working range of the electrodes, the linearity of the modified electrodes was $5 \times 10^{-6} - 1 \times 10^{-1}$ M and was stable for each measurement for the modified electrodes, as the linearity range shortened for the GCE/ISM. The presence of the PPer significantly improved the long-term stability (E^0). The intermediate layer with the smallest thickness proved to be the best modification in this case, which gave the best measurement repeatability. The GCE/10c_PPer/ISM had the best stability, as evidenced by the low value of the standard deviation determined for E^0 values from all measurements (SD= 1.10 mV) and a potential drift equal to 0.015 mV/day (both parameters were more than 50 times better than for unmodified electrodes). The potential drift E^0 for the other electrodes was 1.305, 0.431, and 0.266 mV/day, respectively for GCE/ISM, GCE/20c_PPer/ISM, and GCE/30c_PPer/ISM. The presence of the perinone polymer resulted in sensational long-term stability - the E^0 value improved the most for the electrode with PPer applied at 10 cycles. Compared to the electrode GCE/10c_PPer/ISM, a slightly worse stability was observed for the GCE/20c_PPer/ISM and GCE/30c_PPer/ISM. However, the potential drift and SD values obtained for these electrodes were still much lower than for the electrode without the PPer layer.

3.4. Reversibility and short-term stability of the potential

To check the effectiveness of the implemented intermediate layer in the obtained electrodes, the short-term potential stability was determined. For this purpose, the potential of the SCISEs was measured in a solution of the KNO_3 solution with a concentration of 1×10^{-3} M for 3 hours. The dependence of the potential on time was determined (Fig. 5), from which the potential drift values were then calculated (potential drift=$\Delta E/\Delta t$; where ΔE – the difference of the initial and final potentials, Δt – the difference of time). The value of this parameter for the tested GCE/ISM, GCE/10c_PPer/ISM, GCE/20c_PPer/ISM, and GCE/30c_PPer/ISM electrodes was 27.1×10^{-4} mV/s, 2.7×10^{-4} mV/s, 6.5×10^{-4} mV/s, and 4.1×10^{-4} mV/s, respectively. All the PPer-modified electrodes showed significantly better stability, indicating a good effect of the introduced interlayer on the parameters of the SCISEs. The lowest potential drift was observed for the electrodes modified with the polymer applied at 10 cycles, which was 10 times lower than that for the GCE/ISM.

To check the reversibility of the potential, measurements were conducted in 1×10^{-4} M and 1×10^{-3} M KNO_3 solutions, alternately. The procedure for measuring potentials at different concentrations was repeated five times (Fig. 6). The values of standard deviations for the 5

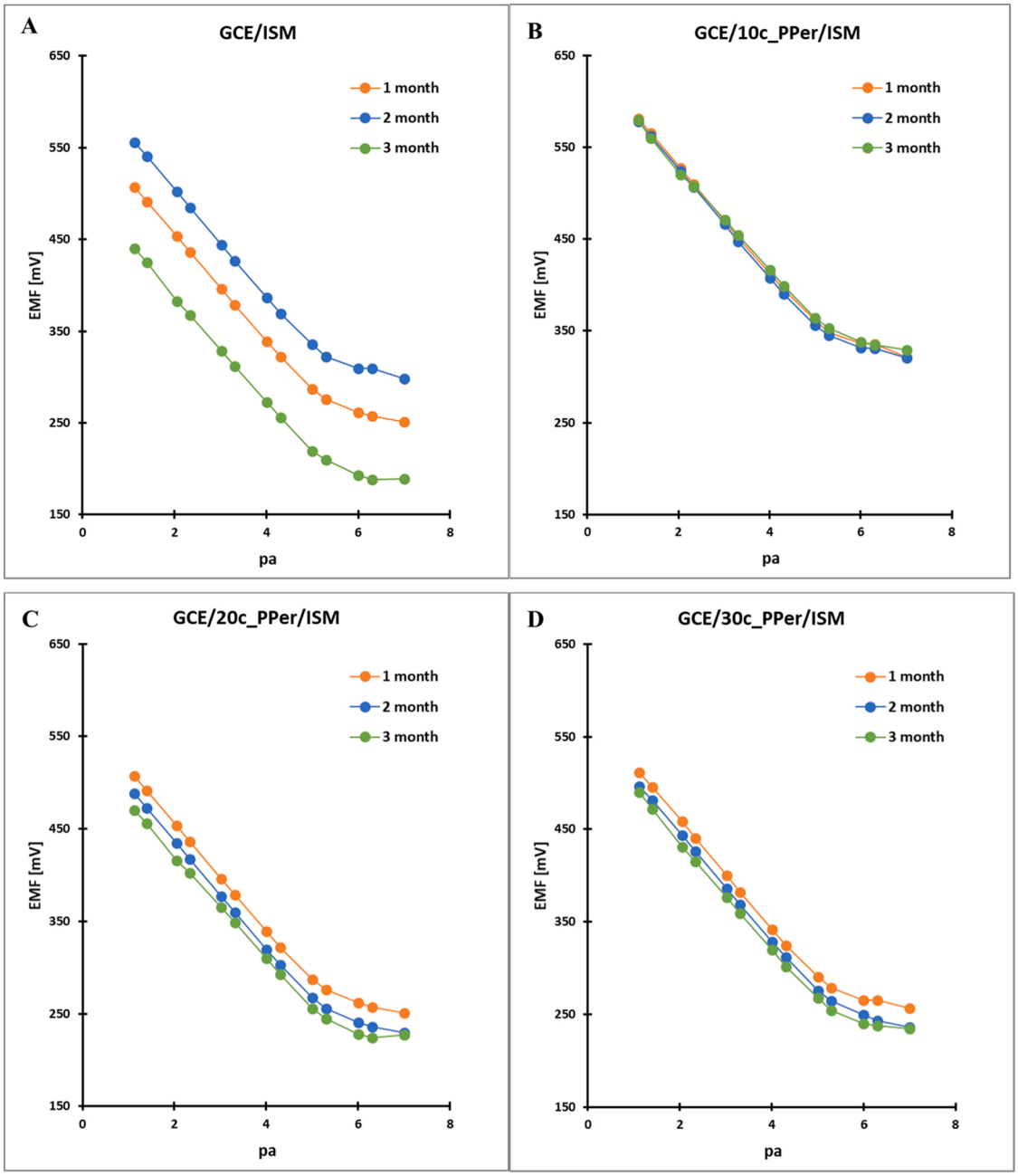

Fig. 4. Compilation of electrode calibration curves from three months of measurements.

measurements at both concentrations are shown in Table 2. The reversibility of the potential turned out to be significantly better for the electrodes modified with PPer. The GCE/10c_PPer/ISM was characterized by the best reversibility, as evidenced by a 26 times lower standard deviation value at the lower concentration and a 10 times lower value at the higher concentration compared to the GCE/ISM. The electrodes in which the polymer was applied at 20 and 30 cycles also showed improved reversibility relative to the unmodified electrode. In this case, the thickness of the intermediate layer affected the described parameter – the thinnest intermediate layer was the best modification option, which resulted in a satisfying reversibility value.

3.5. Selectivity

The next analyzed parameter was selectivity. The potentiometric selectivity coefficients (K_{ij}) were determined using the separate solution method. All electrodes exhibited excellent selectivity behavior, but the electrodes with the intermediate PPer layer showed slightly better values of the selectivity coefficients than the GCE/ISM electrode with regard to almost every interfering ion. Only in the case of ammonium cations for the unmodified electrode were the results very similar to those obtained for the other sensors. The low values of the logarithmic selectivity coefficients confirm the good selectivity of the proposed ion-sensitive membrane (Table S1).

3.6. Effect of light and gases

In order to check whether changing lighting affects the potential of the tested electrodes GCE/ISM, GCE/10c_PPer/ISM, GCE/20c_PPer/ISM and GCE/30c_PPer/ISM, alternating measurements were carried out in the light and the dark, in 1×10^{-3} M KNO_3. The illumination intensity had a little effect on the potential stability of all electrodes, regardless of

Table 1
Selected parameters of the SCISEs variable over 3 months.

SCISE	Slope [mV/decade] (1 month)	Slope [mV/decade] (2 month)	Slope [mV/decade] (3 month)	Detection limit [μM] (1 month)	Detection limit [μM] (2 month)	Detection limit [μM] (3 month)	Linearity range [M] (1 month)	Linearity range [M] (2 month)	Linearity range [M] (3 month)	$E^0 \pm SD$ [mV] (SD from average value for n=12)
GCE/ISM	57.40	57.77	56.22	2.71	3.72	5.00	5×10^{-6}–1×10^{-1}	1×10^{-5}–1×10^{-1}	1×10^{-5}–1×10^{-1}	564.20 ± 58.95
GCE/10c_PPer/ISM	58.89	58.86	58.86	1.23	1.28	1.30	5×10^{-6}–1×10^{-1}	5×10^{-6}–1×10^{-1}	5×10^{-6}–1×10^{-1}	644.02 ± 1.10
GCE/20c_PPer/ISM	56.98	57.64	57.32	2.52	2.52	2.69	5×10^{-6}–1×10^{-1}	5×10^{-6}–1×10^{-1}	5×10^{-6}–1×10^{-1}	551.29 ± 15.02
GCE/30c_PPer/ISM	57.79	57.58	57.68	2.23	1.99	1.82	5×10^{-6}–1×10^{-1}	5×10^{-6}–1×10^{-1}	5×10^{-6}–1×10^{-1}	562.46 ± 12.01

the presence and thickness of the PPer modifying layer.

To check whether the presence of oxygen and carbon dioxide caused a change in the potential stability of the SCISEs, measurements were carried out in 1×10^{-3} M of the KNO_3 solution. Measurements were made alternately for 3 minutes in the solution saturated with the gases mentioned above and the solution through which a stream of nitrogen was passed for 20 minutes before each measurement (Fig. 7). The electrodes with the conductive polymer intermediate layer had stable potentials in both solutions. For the GCE/ISM electrode, an unfavorable potential drift was observed toward higher potentials.

3.7. Water layer test

The electrodes were checked for the formation of a water layer[54]. Fig. 8 shows the pattern of potential changes recorded for the GCE/ISM and GCE/10c_PPer/ISM. In the case of GCE/ISM, after changing the solution from the main to the interfering ion, significant potential fluctuations were observed. When the interfering ion was changed to the main ion, the electrode potential had a different value from that in the same solution but before contact with the interfering ions (the difference was 40 mV). The electrode's indications were also not stable over time since a constant negative potential drift was observed, which demonstrates the formation of a water layer. Different results were recorded for the modified electrodes. The record of potential changes for the GCE/10c_PPer/ISM shows that no potential drift can be seen during both solution changes. The GCE/10c_PPer/ISM electrode, even after several hours of measurement in a sodium solution, gave a reproducible potential for the main ion (the difference between the final potential for the first measurement and the initial potential for the second measurement was 0.408 mV), which was stable over time during the 20-hour measurement (a potential drift that was 100 times smaller than that for the GCE/ISM). Similar results of the aqueous layer test were obtained for the other two electrodes modified with PPer.

3.8. Electrochemical impedance spectroscopy measurements

Electrochemical impedance spectroscopy (EIS) was used to determine the electrical parameters of the electrodes. The obtained impedance spectra are shown in Fig. 9. For all electrodes with a polymer membrane, characteristic impedance spectra were obtained, which are characterized by the presence of a semicircle recorded for high frequencies (this describes the resistance of the ion-selective membrane (R_b) and its bulk capacitance) and a branch forming a certain part of the second semicircle, defining the double layer capacitance and the charge transfer resistance between the membrane and the substrate electrode [5,55,56]. Based on the analysis of the presented spectra, we see that in terms of shape, they do not differ fundamentally. At the same time, we can see the difference in the size of the individual parts of the spectrum, which is due to the different values of the electrical parameters. These were determined by matching the equivalent circuit shown in the insert of Fig. 9. The obtained data are shown in Table 3, where it can be seen that the lowest value of membrane resistance (R_b) was obtained for the GCE/10c_PPer/ISM, equal to 286 kΩ, while the values for the other modified electrodes were higher – 1640 and 1140 kΩ for the GCE/20c_PPer/ISM and GCE/30c_PPer/ISM, respectively. As can be seen, the resistance value of the membrane depends on the number of cycles of the applied PPer polymer. This is related to the deposited PPer layer's surface form and the membrane's different penetrations into the polymer layer. The PPer layer deposited at 10 cycles was characterized by the highest roughness and therefore the membrane penetrating into its structure reduces its resistance to the greatest extent. The growth of the perinone polymer layer results in a more flattened structure. In this case, the amount of membrane layer penetrating into the structure of the PPer layer is reduced and the membrane resistance is increased in accordance with the degree of roughness of the PPer layer [57]. However, in each case, the introduction of an intermediate layer resulted in a

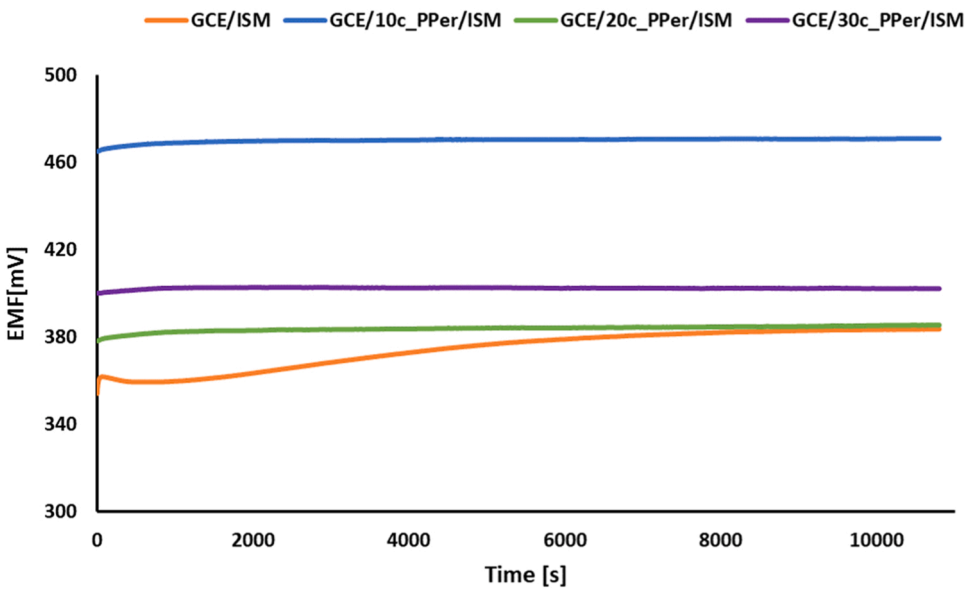

Fig. 5. The short-term stability of the potential.

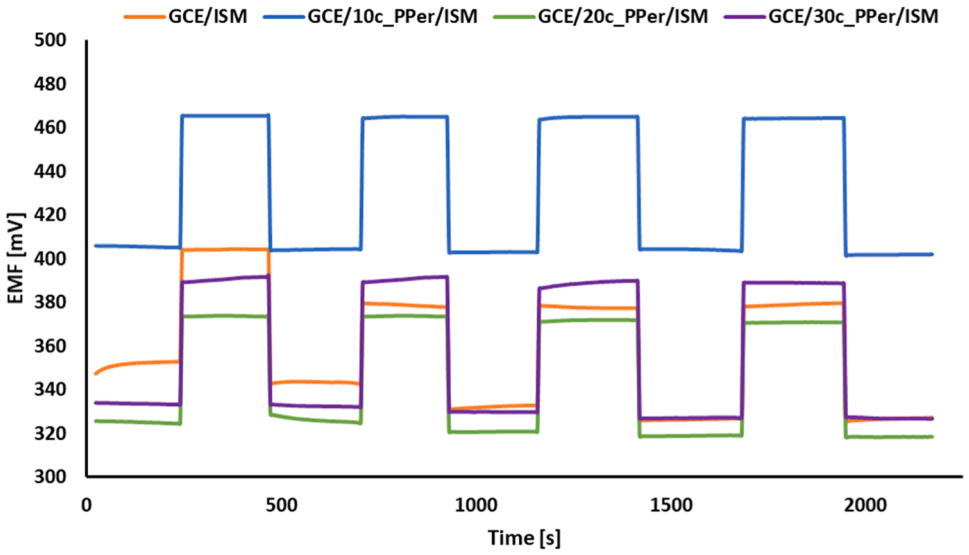

Fig. 6. Reversibility of the potential of the SCISEs.

Table 2
Results of reversibility measurements, mean potential values and standard deviation determined in 1×10^{-3} M and 1×10^{-4} M KNO_3.

SCISE	Mean EMF ±SD for 1×10^{-3} M (n=5) [mV]	Mean EMF ±SD for 1×10^{-4} M (n=5) [mV]
GCE/ISM	384.97 ± 12.69	335.35 ± 11.29
GCE/10c_PPer/ISM	464.89 ± 0.31	403.90 ± 0.78
GCE/20c_PPer/ISM	375.42 ± 1.31	321.25 ± 2.79
GCE/30c_PPer/ISM	388.95 ± 1.02	330.44 ± 1.63

decrease in the membrane resistance since the value of the R_b parameter obtained for the GCE/ISM electrode was 2040 kΩ. The introduced intermediate layer improved the process of charge transfer between the membrane and the substrate material, as evidenced by the significantly reduced charge transfer resistance for the modified electrodes compared to the unmodified electrode and the higher value of electrical capacitance for each electrode against the unmodified electrode. This is undoubtedly related to the specific surface area of the tested layers - the larger the specific surface area, the greater the electrical capacitance. As we can see, there is no proportional value as regards the thickness of the layers – the rule the thicker the layer the better is not correct here. The best modification was the introduction of a polymer layer by a 10-cycle electrodeposition. In this case, the highest roughness was obtained, and thus the highest specific surface area and electrical capacitance. Therefore, the membrane-intermediate layer contact area increased and the resistance decreased. As a result, we obtained the best values of the electrical parameters for this modification. In terms of these parameters, the next electrode was the GCE/30c_PPer/ISM. The electrode in which the polymer was applied at 20 cycles turned out to be worse in terms of the resistance and electrical capacitance of the double layer. This is correlated precisely with the aforementioned roughness – due to the lower heterogeneity of the intermediate layer surface of the

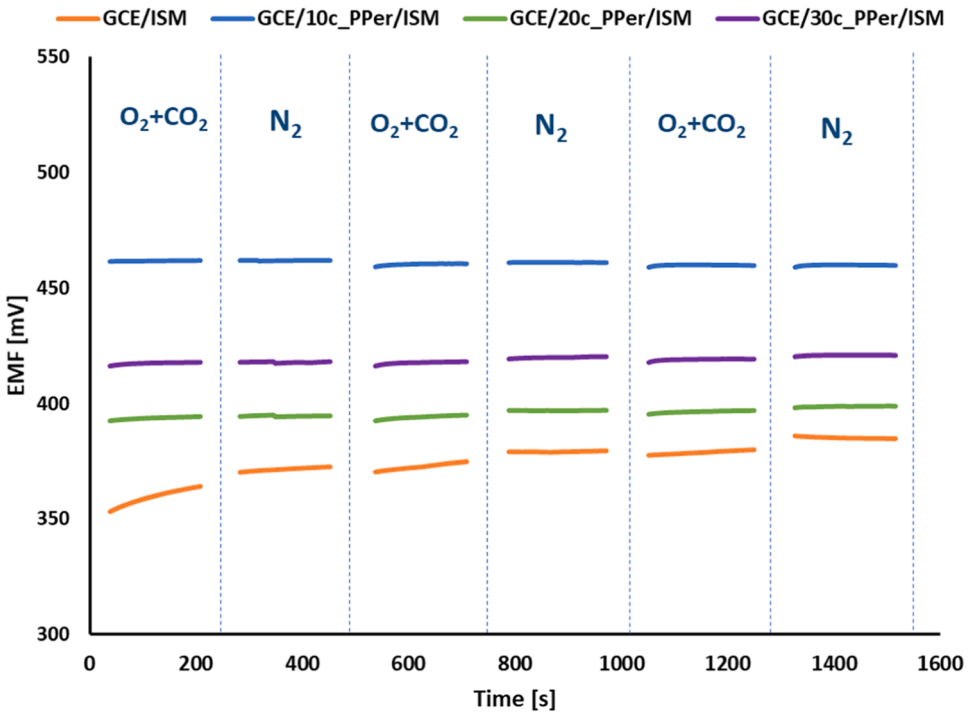

Fig. 7. The influence of gases on the potential.

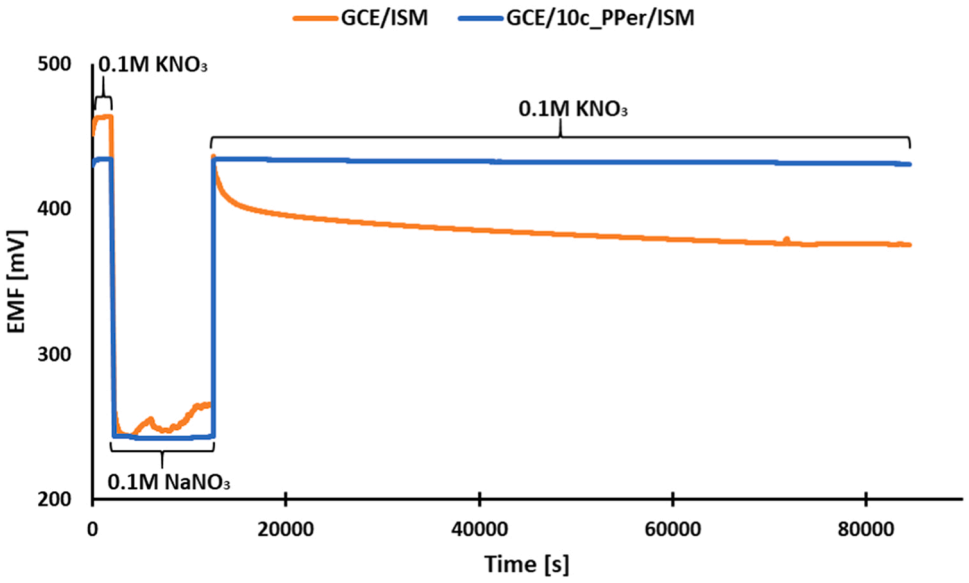

Fig. 8. The results of the water layer test for the GCE/ISM and GCE/10c_PPer/ISM.

GCE/20c_PPer/ISM electrode, weaker results of the electrical parameters were obtained for the GCE/30c_PPer/ISM electrode.

R_u, uncompensated series resistance; R_b, bulk resistance; R_{ct}, charge transfer resistance; CPE, constant phase element; Y^0, initial value for the admittance for the CPE element; N, parameter showing to what extent the CPE is the ideal capacitance (if N= 1, then the CPE is the ideal capacitance, and when N= 0.5, it is Warburg impedance).

3.9. Chronopotentiometry measurements

The chronopotentiometry technique was used to determine the potential stability under current conditions and electrical capacitance. The chronopotentiograms obtained for the GCE/ISM (applied current 10 nA) and the GCE/10c_PPer/ISM (applied current 100 nA) are shown in Fig. 10. By using the received data the potential drift was determined from the slope of the linear part of E-t curves and the electrical capacitance was evaluated from the dependence C=i/(dE/dt) (where: E – measured potential, i – value of the applied current, t-time, C - electrical capacitance) [57]. The values of potential drift equal to 1740, 310, 627, and 405 μV/s (for GCE/ISM, GCE/10c_PPer/ISM, GCE/20c_PPer/ISM, GCE/30c_PPer/ISM, respectively) were determined, as well as the values of electrical capacitance equal to 5.75, 322, 159 and 246 μF (for the same order of electrodes). For the PPer based electrodes the capacitance increases with the increase of the PPer layer roughness. Similar results were observed in the paper [58]. As was expected, the PPer interlayer electrodes exhibited higher electrical capacitance, compared to simple

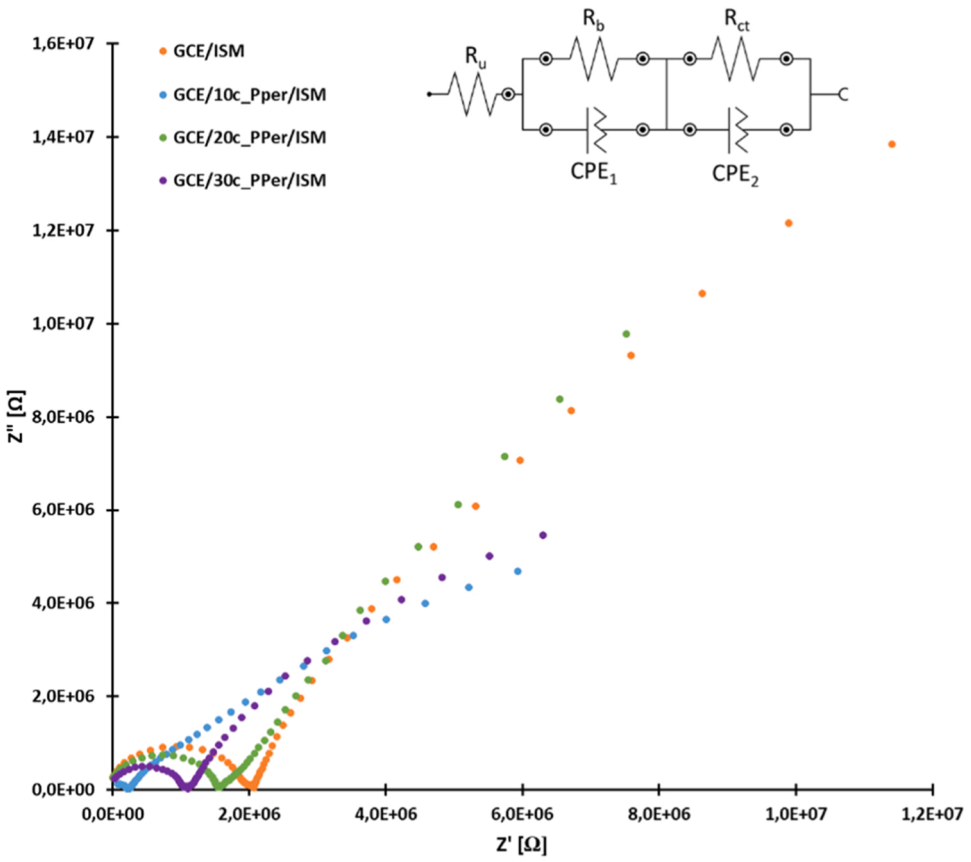

Fig. 9. The impedance spectra of the tested SCISEs.

Table 3
The determined values of the electrical parameters.

Electrode	R_u [kΩ]	R_b [kΩ]	CPE_1 Y^0 (N), [pF]	R_{ct} [kΩ]	CPE_2 Y^0 (N), [μF]
GCE/ISM	67.6	2040	16.0(0.92)	90000	0.38(0.74)
GCE/ 10c_PPer/ ISM	56.1	286	45.3(0.84)	18900	0.54(0.62)
GCE/ 20c_PPer/ ISM	45,3	1640	13.2(0.94)	65000	0.59(0.72)
GCE/ 30c_PPer/ ISM	57.8	1140	20.6(0.90)	22300	0.77(0.72)

glassy carbon disc electrodes coated only with a potassium membrane. As a result, the modified electrodes exhibited significantly smaller potential drifts than unmodified electrodes.

3.10. Comparison of the parameters for the tested GCE/10c_PPer/ISM and other SCISEs modified with using single solid contact material

Table 4 presents a comparison of parameters for potassium ion-selective electrodes that differ in the type of used solid contact. The solid contact was composed of a single material, such as a conductive polymer. These included poly(3-octylthiophene) (POT)[59], polyaniline (PANI)[60,61], poly(3,4-ethylenedioxythiophene) (PEDOT)[57], polypyrrole (PPy)[62], and the perinone polymer (PPer) presented in this study. Additionally, the table highlights the use of polypyrrole films doped with perfluorooctanesulfonate (PPy-PFOS)[35] as SCs. The table also demonstrates that conductive polymers are not the only materials utilized as SCs. Other examples include carbon-based materials such as C60[63], three-dimensionally ordered macroporous carbon (3DOM) [64], and graphene[65,66], as well as metal oxide nanoparticles like MoO_2[67]. Most of the electrodes featured glassy carbon electrodes as the inner electrode, while platinum (Pt) was used in this role in two cases. The electrode developed by our research team exhibited a slope close to the Nernstian value, and it demonstrated higher sensitivity compared to other polymer-based SCs, such as PANI, PEDOT, PPy, and PPy-PFOS, as well as carbon-based materials. Compared to the aforementioned electrodes, the GCE/10c_PPer/ISM electrode had a fairly wide working range. The detection limits of these electrodes were very close. A remarkable advantage of the GCE/10c_PPer/ISM electrode is its superior long-term potential stability, which is made possible by the use of perinone polymer as a solid contact layer, providing better ion-electron conductivity between the membrane and the inner electrode. As a result, during three months of use the electrode did not become damaged and provided similar potential values, as indicated by the low short-term and excellent long-term stability.

4. Conclusions

This paper describes the use of a new perinone polymer (PPer) as a solid contact in ion-selective electrodes. The advantage of the proposed polymer is its amphiphilic nature, which increases adhesion both to the phase of the electrode substrate (aromatic segments and partial ladder) and to the ion-sensitive membrane (stable redox centers of the polymer with trapped ions). It has favorable electrical properties (a mixed nature of conductivity and a wide charging current in a very large potential range) and acts effectively as a solid contact. The PPer was deposited by simple potentiodynamic technique onto the surface of the electrode substrate in three modes differing in the number of cycles. Such modification resulted in a significant improvement in the performance of the tested sensors. The most promising results were obtained for the GCE/

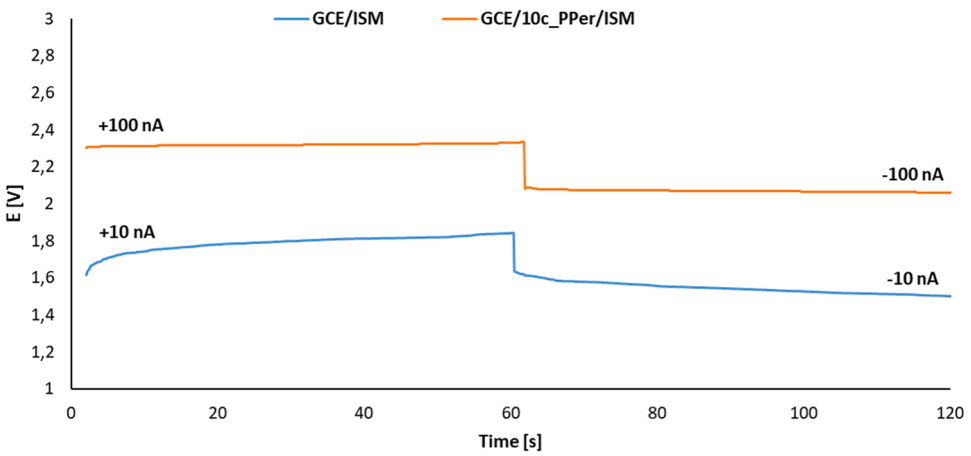

Fig. 10. Chronopotentiograms for GCE/ISM and GCE/10c_PPer/ISM.

Table 4
Comparison of selected parameters of the tested electrode modified with perinone polymer with other potassium electrodes.

Solid contact material	Type of Internal Electrode	Slope [mV/decade]	Range of Linearity [M]	Limit of Detection [M]	Potential stability		Reference
					Short-term [μV/s]	Long-term [mV/day]	
POT	GCE	59.2	5.0×10^{-7}–1.0×10^{-1}	1.0×10^{-7}	N/A	N/A	[59]
PANI	GCE	58.2	1.0×10^{-5}–1.0×10^{-1}	N/A	N/A	Pure stability	[60]
PANI	Pt	58.2	1.0×10^{-5}–1.0×10^{-1}	6.3×10^{-6}	N/A	N/A	[61]
PEDOT	GCE	56.3	1.0×10^{-4}–1.0×10^{-1}	N/A	4.9 (i=1 nA)	N/A	[57]
PPy	Pt	51.0	6.0×10^{-6}–1.0×10^{-1}	1.8×10^{-6}	N/A	N/A	[62]
C60	GCE	58.9	1.0×10^{-5}–1.0×10^{-1}	N/A	N/A	N/A	[63]
3DOM	GCE	N/A	7.5×10^{-6}–1.0×10^{-3}	6.3×10^{-7}	N/A	0.28	[64]
Graphene	GCE	58.3	1.0×10^{-5}–1.0×10^{-1}	1.0×10^{-6}	38.5 (i=10 nA)	N/A	[65]
Graphene	GCE	58.4	1.6×10^{-6}–1.0×10^{-1}	6.3×10^{-7}	12.8 (i=1 nA)	0.14	[66]
MoO_2	GCE	55.0	1.0×10^{-5}–1.0×10^{-2}	3.2×10^{-6}	11.7 (i=1 nA)	Good (not data)	[67]
PPy-PFOS	GCE	57.0	1.0×10^{-6}–1.0×10^{-2}	8.8×10^{-8}	0.019 (i=0)	1.66	[35]
PPer	**GCE**	**58.9**	**5.0×10^{-6}–1.0×10^{-1}**	**1.23×10^{-6}**	**0.27 (i=0)**	**0.015**	**This work**

10c_PPer/ISM electrode, in which the solid contact PPer layer was applied in 10 cycles. The obtained electrode exhibited the highest sensitivity of 58.86 mV/decade and also had the best repeatability of results over time.

In introducing an intermediate layer, our main goal was to improve the stability and reversibility of the potential of the SCISEs. The presence of the intermediate layer significantly improved these parameters, as evidenced by the significantly lower potential drift and significantly lower SD values for the potentials measured in both 1×10^{-4} M and 1×10^{-3} M KNO_3 solution for the electrodes with the PPer solid contact than for the unmodified electrode. In the case of selectivity, the presence and thickness of the intermediate layer did not significantly affect this parameter. After checking the resistance of the electrodes to external factors such as light and the presence of gases, the conclusion was reached that the presence of polymeric layers minimized the influence of the external environment on their potential, resulting in a stable potential for each layer thickness. An additional advantage of the modified electrodes is their stable design and structure, inside which no water layer is formed, which would cause the stable and reversible potential to deteriorate during use, whereas the potential drift would become more troublesome, which would translate into inaccurate and unreliable results. The stability and reversibility of the potential are closely related to electrical parameters, i.e. the electrical capacitance of the double layer, the resistance of the membrane, and the resistance of the charge transfer between the ion-selective membrane and the inner electrode. The implementation of PPer in 10 cycles allowed us to obtain 6 times lower membrane resistance and almost 5 times lower charge transfer resistance, which is clear evidence that the introduction of a layer consisting of PPer with a developed surface and conducting properties is a good modification solution in SCISEs.

Funding

The authors acknowledge funding from the Polish National Science Centre (NCN) (project *No.* 2021/41/B/ST5/03221). This research was also supported under the Excellence Initiative – Research University programme at the Silesian University of Technology in Gliwice (grants No. 32/014/RGJ22/2007, 04/040/RGJ23/0238, and 04/040/RGJ23/0242).

CRediT authorship contribution statement

Klaudia Morawska: Writing – original draft, Validation, Investigation, Formal analysis, Data curation, Conceptualization. **Mieczyslaw Lapkowski:** Writing – review & editing, Resources, Funding acquisition. **Cecylia Wardak:** Writing – review & editing, Supervision, Resources, Methodology, Conceptualization. **Malgorzata Czichy:** Writing – review & editing, Resources, Methodology, Funding acquisition. **Patryk Janasik:** Writing – review & editing, Methodology.

Declaration of Competing Interest

The authors declare the following financial interests/personal relationships which may be considered as potential competing interests: Malgorzata Czichy, Mieczyslaw Lapkowski reports financial support was provided by Polish National Science Centre. Mieczyslaw Lapkowski,

Patryk Janasik, Malgorzata Czichy has patent #P.441371 pending to Silesian University of Technology. Mieczyslaw Lapkowski, Patryk Janasik, Malgorzata Czichy has patent #EPO EP22460052 pending to Silesian University of Technology. If there are other authors, they declare that they have no known competing financial interests or personal relationships that could have appeared to influence the work reported in this paper.

Data availability

Data will be made available on request.

Acknowledgment

Special thanks from the author (Klaudia Morawska) to the Silesian University of Technology for the internship opportunity, synthesis of perinone precursors, and the possibility of participating in processes such as the electropolymerization process of the perinone polymer. This work is partially supported by the Polish National Science Centre and under the Excellence Initiative – Research University programme at the Silesian University of Technology in Gliwice.

Appendix A. Supporting information

Supplementary data associated with this article can be found in the online version at doi:10.1016/j.snb.2024.136662.

References

[1] Y. Lyu, S. Gan, Y. Bao, L. Zhong, J. Xu, W. Wang, Z. Liu, Y. Ma, G. Yang, L. Niu, Solid-contact ion-selective electrodes: response mechanisms, transducer materials and wearable sensors, Membranes 10 (2020) 128, https://doi.org/10.3390/membranes10060128.

[2] C. Wardak, Solid contact nitrate ion-selective electrode based on ionic liquid with stable and reproducible potential, Electroanalysis 26 (2014) 864–872, https://doi.org/10.1002/elan.201300590.

[3] K. Węgrzyn, A. Michalska, K. Maksymiuk, Electrochemical properties and analytical advantages of potassium-selective sensor with tungsten trioxide solid contact, J. Electroanal. Chem. 928 (2023) 117061, https://doi.org/10.1016/j.jelechem.2022.117061.

[4] W. Jiang, C. Liu, Y. Zhao, G.I.N. Waterhouse, Z. Zhang, L. Yu, A solid-contact Pb2+-selective electrode based on a hydrophobic polyaniline microfiber film as the ion-to-electron transducer, Synth. Met 248 (2019) 94–101, https://doi.org/10.1016/j.synthmet.2019.01.008.

[5] C. Wardak, K. Pietrzak, K. Morawska, Nanocomposite of copper oxide nanoparticles and multi-walled carbon nanotubes as a solid contact of a copper-sensitive ion-selective electrode: intermediate layer or membrane component–comparative studies, Appl. Nanosci. (2023), https://doi.org/10.1007/s13204-023-02846-x.

[6] J. Zhu, X. Li, Y. Qin, Y. Zhang, Single-piece solid-contact ion-selective electrodes with polymer–carbon nanotube composites, Sens Actuators B Chem. 148 (2010) 166–172, https://doi.org/10.1016/j.snb.2010.04.041.

[7] K.R. Choi, B.K. Troudt, P. Bühlmann, Ion-selective electrodes with sensing membranes covalently attached to both the inert polymer substrate and conductive carbon contact, Angew. Chem. 135 (2023), https://doi.org/10.1002/ange.202304674.

[8] K. Pietrzak, K. Morawska, S. Malinowski, C. Wardak, Chloride ion-selective electrode with solid-contact based on polyaniline nanofibers and multiwalled carbon nanotubes nanocomposite, Membranes 12 (2022) 1150, https://doi.org/10.3390/membranes12111150.

[9] J. Bobacka, Conducting polymer-based solid-state ion-selective electrodes, Electroanalysis 18 (2006) 7–18, https://doi.org/10.1002/elan.200503384.

[10] K. Pietrzak, C. Wardak, S. Malinowski, Application of polyaniline nanofibers for the construction of nitrate all-solid-state ion-selective electrodes, Appl. Nanosci. 11 (2021) 2823–2835, https://doi.org/10.1007/s13204-021-02228-1.

[11] P. Wang, H. Liu, S. Zhou, L. Chen, S. Yu, J. Wei, A review of the carbon-based solid transducing layer for ion-selective electrodes, Molecules 28 (2023) 5503, https://doi.org/10.3390/molecules28145503.

[12] J. Kozma, S. Papp, R.E. Gyurcsányi, Solid-contact ion-selective electrodes based on ferrocene-functionalized multi-walled carbon nanotubes, Electrochem Commun. 123 (2021) 106903, https://doi.org/10.1016/j.elecom.2020.106903.

[13] C. Wardak, K. Morawska, B. Paczosa-Bator, M. Grabarczyk, Improved lead sensing using a solid-contact ion-selective electrode with polymeric membrane modified with carbon nanofibers and ionic liquid nanocomposite, Materials 16 (2023) 1003, https://doi.org/10.3390/ma16031003.

[14] N. Lenar, B. Paczosa-Bator, R. Piech, Ruthenium dioxide nanoparticles as a high-capacity transducer in solid-contact polymer membrane-based pH-selective electrodes, Microchim. Acta 186 (2019) 777, https://doi.org/10.1007/s00604-019-3830-x.

[15] K. Pietrzak, N. Krstulović, D. Blažeka, J. Car, S. Malinowski, C. Wardak, Metal oxide nanoparticles as solid contact in ion-selective electrodes sensitive to potassium ions, Talanta 243 (2022) 123335, https://doi.org/10.1016/j.talanta.2022.123335.

[16] N. Lenar, R. Piech, C. Wardak, B. Paczosa-Bator, Application of metal oxide nanoparticles in the field of potentiometric sensors: a review, Membranes 13 (2023) 876, https://doi.org/10.3390/membranes13110876.

[17] R. Mobin, T.A. Rangreez, H.T.N. Chisti, Inamuddin, M. Rezakazemi, Organic-Inorganic Hybrid Materials and Their Applications, in: 2019: pp. 1135–1156. https://doi.org/10.1007/978-3-319-95987-0_33.

[18] V.M. Rangaraj, J.-I. Yoo, J.-K. Song, V. Mittal, MOF-derived 3D MnO2@graphene/CNT and Ag@graphene/CNT hybrid electrode materials for dual-ion selective pseudocapacitive deionization, Desalination 550 (2023) 116369, https://doi.org/10.1016/j.desal.2023.116369.

[19] C. Wardak, K. Pietrzak, K. Morawska, M. Grabarczyk, Ion-selective electrodes with solid contact based on composite materials: a review, Sensors 23 (2023) 5839, https://doi.org/10.3390/s23135839.

[20] H. Bao, J. Ye, X. Zhao, Y. Zhang, Conductive polymer nanoparticles as solid contact in ion-selective electrodes sensitive to potassium ions, Molecules 28 (2023) 3242, https://doi.org/10.3390/molecules28073242.

[21] A. Ruiz-Gonzalez, K.L. Choy, Highly selective and robust nanocomposite-based sensors for potassium ions detection, Appl. Mater. Today 23 (2021) 101008, https://doi.org/10.1016/j.apmt.2021.101008.

[22] M. Łapkowski, Perinone—new life of an old molecule, Materials 14 (2021) 6880, https://doi.org/10.3390/ma14226880.

[23] R.L. Van Deusen, Benzimidazo-benzophenanthroline polymers, J. Polym. Sci. B 4 (1966) 211–214, https://doi.org/10.1002/pol.1966.110040310.

[24] M. Mamada, C. Pérez-Bolívar, P. Anzenbacher, Green synthesis of polycyclic benzimidazole derivatives and organic semiconductors, Org. Lett. 13 (2011) 4882–4885, https://doi.org/10.1021/ol201973w.

[25] M. Mamada, C. Pérez-Bolívar, D. Kumaki, N.A. Esipenko, S. Tokito, P. Anzenbacher, Benzimidazole derivatives: synthesis, physical properties, and n-type semiconducting properties, Chem. – A Eur. J. 20 (2014) 11835–11846, https://doi.org/10.1002/chem.201403058.

[26] N. Lenar, B. Paczosa-Bator, R. Piech, A. Królicka, Poly(3-octylthiophene-2,5-diyl) - nanosized ruthenium dioxide composite material as solid-contact layer in polymer membrane-based K+-selective electrodes, Electro Acta 322 (2019) 134718, https://doi.org/10.1016/j.electacta.2019.134718.

[27] N. Lenar, R. Piech, B. Paczosa-Bator, Hydrous cerium dioxide-based materials as solid-contact layers in potassium-selective electrodes, Membranes 12 (2022) 349, https://doi.org/10.3390/membranes12040349.

[28] S. Manandhar, V. Yrjänä, I. Leito, J. Bobacka, Determination of benzoate in cranberry and lingonberry by using a solid-contact benzoate-selective electrode, Talanta 274 (2024) 125996, https://doi.org/10.1016/j.talanta.2024.125996.

[29] T. Yamada, K. Kanda, Y. Yanagida, G. Mayanagi, J. Washio, N. Takahashi, All-solid-state fluoride ion-selective electrode using LaF_3 single crystal with poly(3,4-ethylenedioxythiophene) as solid contact layer, Electroanalysis 35 (2023), https://doi.org/10.1002/elan.202200103.

[30] C. Bahro, S. Goswami, S. Gernhart, D. Koley, Calibration-free solid-state ion-selective electrode based on a polarized PEDOT/PEDOT-S-doped copolymer as back contact, Anal. Chem. 94 (2022) 8302–8308, https://doi.org/10.1021/acs.analchem.2c00748.

[31] X. Zeng, Y. Liu, G.I.N. Waterhouse, X. Jiang, Z. Zhang, L. Yu, Porous three-dimensional poly(3,4-ethylenedioxythiophene)/K3Fe(CN)6 network as the solid contact layer in high stability Pb2+ ion-selective electrodes, Microchem. J. 177 (2022) 107279, https://doi.org/10.1016/j.microc.2022.107279.

[32] H. Li, M.E. DeCoster, C. Ming, M. Wang, Y. Chen, P.E. Hopkins, L. Chen, H.E. Katz, Enhanced molecular doping for high conductivity in polymers with volume freed for dopants, Macromolecules 52 (2019) 9804–9812, https://doi.org/10.1021/acs.macromol.9b02048.

[33] W. Hayes, B.W. Greenland, Donor–Acceptor π–π Stacking Interactions: From Small Molecule Complexes to Healable Supramolecular Polymer Networks, in: 2015: pp. 143–166. https://doi.org/10.1007/978-3-319-15404-6_4.

[34] R. Gracia, D. Mecerreyes, Polymers with redox properties: materials for batteries, biosensors and more, Polym. Chem. 4 (2013) 2206, https://doi.org/10.1039/c3py21118e.

[35] N. He, S. Papp, T. Lindfors, L. Höfler, R.M. Latonen, R.E. Gyurcsányi, Pre-polarized hydrophobic conducting polymer solid-contact ion-selective electrodes with improved potential reproducibility, Anal. Chem. 89 (2017) 2598–2605, https://doi.org/10.1021/acs.analchem.6b04885.

[36] E. Lindner, B.P. Hambly, C.K. Sears, M. Guzinski, F. Perez, R.M. Latonen, J. Bobacka, B.D. Pendley, Multilayer and surface immobilization of EDOT-decorated nanocapsules, Langmuir (2021), https://doi.org/10.1021/acs.langmuir.0c03160.

[37] J. Kozma, S. Papp, R.E. Gyurcsányi, Highly hydrophobic TEMPO-functionalized conducting copolymers for solid-contact ion-selective electrodes, Bioelectrochemistry 150 (2023), https://doi.org/10.1016/j.bioelechem.2022.108352.

[38] N. Lenar, R. Piech, B. Paczosa-Bator, Carbon nanomaterials - Poly(3-octylthiophene-2,5-diyl) – hydrous iridium dioxide triple composite materials as superhydrophobic layers for ion-selective electrodes, J. Electrochem Soc. 169 (2022) 127508, https://doi.org/10.1149/1945-7111/aca838.

[39] S. Erten, S. Icli, Bilayer heterojunction solar cell based on naphthalene bis-benzimidazole, Inorg. Chim. Acta 361 (2008) 595–600, https://doi.org/10.1016/j.ica.2007.02.047.
[40] C. Tozlu, S. Erten-Ela, S. Icli, Photoresponsive n-channel organic field effect transistor based on naphthalene bis-benzimidazole with divinyltetramethyl disiloxane-bis (benzo-cyclobutene) gate insulator, Sens Actuators A Phys. 161 (2010) 46–52, https://doi.org/10.1016/j.sna.2010.05.030.
[41] J. Mizuguchi, Crystal Structure and Electronic Characterization of *trans* - and *cis* -Perinone Pigments, J. Phys. Chem. B 108 (2004) 8926–8930, https://doi.org/10.1021/jp031351d.
[42] J.L. Teteruk, J. Glinnemann, W. Heyse, K.E. Johansson, J. van de Streek, M. U. Schmidt, Local structure in the disordered solid solution of *cis* - and *trans* -perinones, Acta Crystallogr B Struct. Sci. Cryst. Eng. Mater. 72 (2016) 416–433, https://doi.org/10.1107/S2052520616004972.
[43] D.A. Zherebtsov, M.U. Schmidt, R. Niewa, C.P. Sakthidharan, F.V. Podgornov, Y. V. Matveychuk, S.A. Nayfert, M.A. Polozov, S.N. Ivashevskaya, A.I. Stash, Y.-S. Chen, D.E. Zhivulin, V.E. Zhivulin, S.V. Merzlov, E.V. Bartashevich, V.V. Avdin, H.S. Hsu, F.W. Guo, Two new polymorphs of *cis* -perinone: crystal structures, physical and electric properties, Acta Crystallogr B Struct. Sci. Cryst. Eng. Mater. 75 (2019) 384–392, https://doi.org/10.1107/S2052520619003287.
[44] M. Czichy, R. Motyka, P. Zassowski, E. Grabiec, P. Janasik, A. Brzeczek-Szafran, K. Laba, A. Wolinska-Grabczyk, M. Lapkowski, Effects of solution-phase ordering on the spectroscopic properties and electrooxidative reactivity of isomeric mixtures and isolated isomers of synthesized amidine derivatives, Dyes Pigments 178 (2020) 108309, https://doi.org/10.1016/j.dyepig.2020.108309.
[45] M. Czichy, P. Janasik, P. Wagner, D.L. Officer, M. Lapkowski, Electrochemical and spectroelectrochemical studies on the reactivity of perimidine–carbazole–thiophene monomers towards the formation of multidimensional macromolecules versus stable π-dimeric states, Materials 14 (2021) 2167, https://doi.org/10.3390/ma14092167.
[46] J.F. Lee, S.L.C. Hsu, P.I. Lee, H.Y. Chuang, M.L. Yang, J.S. Chen, W.Y. Chou, Low bandgap carbazole copolymers containing an electron-withdrawing side chain for solar cell applications, Sol. Energy Mater. Sol. Cells 95 (2011) 2795–2804, https://doi.org/10.1016/j.solmat.2011.05.029.
[47] C. Tamuly, N. Barooah, M. Laskar, R.J. Sarma, J.B. Baruah, Fluorescence quenching and enhancement by h-bonding interactions in some nitrogen containing fluorophores, Supramol. Chem. 18 (2006) 605–613, https://doi.org/10.1080/10610270601045537.
[48] J.R. Palmer, K.A. Wells, J.E. Yarnell, J.M. Favale, F.N. Castellano, Visible-light-driven triplet sensitization of polycyclic aromatic hydrocarbons using thionated perinones, J. Phys. Chem. Lett. 11 (2020) 5092–5099, https://doi.org/10.1021/acs.jpclett.0c01634.
[49] M. Czichy, H. Zhylitskaya, P. Zassowski, M. Navakouski, P. Chulkin, P. Janasik, M. Lapkowski, M. Stępień, Electrochemical polymerization of pyrrole–perimidine hybrids: low-band-gap materials with high n-doping activity, J. Phys. Chem. C. 124 (2020) 14350–14362, https://doi.org/10.1021/acs.jpcc.0c03002.
[50] H. Zhylitskaya, J. Cybińska, P. Chmielewski, T. Lis, M. Stępień, Bandgap engineering in π-extended pyrroles. A modular approach to electron-deficient chromophores with multi-redox activity, J. Am. Chem. Soc. 138 (2016) 11390–11398, https://doi.org/10.1021/jacs.6b07826.
[51] H. Quante, Y. Geerts, K. Müllen, Synthesis of soluble perylenebisamidine derivatives. novel long-wavelength absorbing and fluorescent dyes, Chem. Mater. 9 (1997) 495–500, https://doi.org/10.1021/cm960344h.
[52] P. Janasik, R. Motyka, P. Chulkin, M. Czichy, D. Janasik, J. Vella, C. Tollemache, J. Travas-Sejdic, M. Lapkowski, Electropolymerization and characterization of a new ambipolar perimidine polymer with a perylene core, Electro Acta 487 (2024) 144115, https://doi.org/10.1016/j.electacta.2024.144115.
[53] K. Pietrzak, C. Wardak, Comparative study of nitrate all solid state ion-selective electrode based on multiwalled carbon nanotubes-ionic liquid nanocomposite, Sens Actuators B Chem. 348 (2021) 130720, https://doi.org/10.1016/j.snb.2021.130720.
[54] M. Fibbioli, W.E. Morf, M. Badertscher, N.F. de Rooij, E. Pretsch, Potential drifts of solid-contacted ion-selective electrodes due to zero-current ion fluxes through the sensor membrane, Electroanalysis 12 (2000) 1286–1292, https://doi.org/10.1002/1521-4109(200011)12:16<1286::AID-ELAN1286>3.0.CO;2-Q.
[55] George Horvai, Etelka Graf, Klara Toth, Erno Pungor, R.P. Buck, Plasticized poly (vinyl chloride) properties and characteristics of valinomycin electrodes. 1. High-frequency resistances and dielectric properties, Anal. Chem. 58 (1986) 2735–2740, https://doi.org/10.1021/ac00126a034.
[56] J. Bobacka, A. Ivaska, A. Lewenstam, Plasticizer-free all-solid-state potassium-selective electrode based on poly(3-octylthiophene) and valinomycin, Anal. Chim. Acta 385 (1999) 195–202, https://doi.org/10.1016/S0003-2670(98)00667-9.
[57] J. Bobacka, Potential stability of all-solid-state ion-selective electrodes using conducting polymers as ion-to-electron transducers, Anal. Chem. 71 (1999) 4932–4937, https://doi.org/10.1021/ac990497z.
[58] A. Albina, P.L. Taberna, J.P. Cambronne, P. Simon, E. Flahaut, T. Lebey, Impact of the surface roughness on the electrical capacitance, Microelectron. J. 37 (2006) 752–758, https://doi.org/10.1016/j.mejo.2005.10.008.
[59] K.Y. Chumbimuni-Torres, N. Rubinova, A. Radu, L.T. Kubota, E. Bakker, Solid contact potentiometric sensors for trace level measurements, Anal. Chem. 78 (2006) 1318–1322, https://doi.org/10.1021/ac050749y.
[60] T. Lindfors, A. Ivaska, Stability of the inner polyaniline solid contact layer in all-solid-state K^+ -selective electrodes based on plasticized poly(vinyl chloride), Anal. Chem. 76 (2004) 4387–4394, https://doi.org/10.1021/ac049439q.
[61] W.-S. Han, Y.-H. Lee, K.-J. Jung, S.-Y. Ly, T.-K. Hong, M.-H. Kim, Potassium ion-selective polyaniline solid-contact electrodes based on 4′,4″(5″)-di-tert-butyldibenzo-18-crown-6-ether ionophore, J. Anal. Chem. 63 (2008) 987–993, https://doi.org/10.1134/S1061934808100110.
[62] N. Zine, J. Bausells, F. Vocanson, R. Lamartine, Z. Asfari, F. Teixidor, E. Crespo, I.A. M. de Oliveira, J. Samitier, A. Errachid, Potassium-ion selective solid contact microelectrode based on a novel 1,3-(di-4-oxabutanol)-calix[4]arene-crown-5 neutral carrier, Electro Acta 51 (2006) 5075–5079, https://doi.org/10.1016/j.electacta.2006.03.060.
[63] Z. Mousavi, T. Han, C. Kvarnström, J. Bobacka, A. Ivaska, All-solid-state potassium ion-selective electrode with conducting polymer doped with carbon nanotubes and C60 as the ion-to-electron transducing layers, ECS Trans. 19 (2009) 19–26, https://doi.org/10.1149/1.3118534.
[64] C.-Z. Lai, M.M. Joyer, M.A. Fierke, N.D. Petkovich, A. Stein, P. Bühlmann, Subnanomolar detection limit application of ion-selective electrodes with three-dimensionally ordered macroporous (3DOM) carbon solid contacts, J. Solid State Electrochem. 13 (2009) 123–128, https://doi.org/10.1007/s10008-008-0579-2.
[65] B. Paczosa-Bator, Ion-selective electrodes with superhydrophobic polymer/carbon nanocomposites as solid contact, Carbon N. Y 95 (2015) 879–887, https://doi.org/10.1016/j.carbon.2015.09.006.
[66] J. Ping, Y. Wang, J. Wu, Y. Ying, Development of an all-solid-state potassium ion-selective electrode using graphene as the solid-contact transducer, Electrochem Commun. 13 (2011) 1529–1532, https://doi.org/10.1016/j.elecom.2011.10.018.
[67] X. Zeng, W. Qin, A solid-contact potassium-selective electrode with MoO2 microspheres as ion-to-electron transducer, Anal. Chim. Acta 982 (2017) 72–77, https://doi.org/10.1016/j.aca.2017.05.032.

Klaudia Morawska received the M.Sc. degree in chemistry from Maria Curie Sklodowska University (MCSU), Lublin, Poland, in 2023, where she is currently pursuing the Ph.D. degree with the Department of Analytical Chemistry. Her main scientific interests are research, development, and analytical applications of electrochemical sensors, mainly solid contact ion-selective electrodes based on nanomaterials and composite materials. To date, she has published a dozen peer-reviewed scientific papers. ORCID: 0009–0006–3381–0845.

Malgorzata Czichy received the Ph.D. degree (2009) and D.Sc. degree (2022) in chemical sciences from Silesian University of Technology (Gliwice, Poland). Since 2023, she has been an Associate Professor in the Faculty of Chemistry and also Centre for Organic and Nanohybrid Electronics CONE (Silesian University of Technology). She is the lecturer in the fields of Catalysis, Physical Chemistry and Organic Electronics and the participant of events of popularizing science. She was/is contractor in national and European programmes and PI in national projects. Her areas of interest include (spectro)electrochemistry, electron spin resonance spectroscopy, N-type semiconductors, fullerenes, and (hetero)arene-fused polymers. ORCID: 0000–0002–1441–8163.

Patyk Janasik is a PhD candidate at the Silesian University of Technology, where he also earned his master's degree in chemical technology, specializing in the technology of polymers. His research interests focus on conducting polymers and the electrochemistry of organic compounds. ORCID: 0000–0002–5149-0949.

Mieczyslaw Lapkowski. Professor of Chemistry at Faculty of Chemistry, Silesian University of Technology in Gliwice and Institute of Polymer and Carbon Materials in Zabrze (Poland). He currently is Director of Centre of Organic and Nanohybride Electronics. 1982: Ph.D. in Chemistry at Silesian University of Technology, and second one in 1987 at Université Joseph Fourier, Grenoble (France). 1989: Research Fellow: Oxford University, (GB), 1992: 1993; Invited Professor: l'Université de Nantes, (France) 1994–96, CTE – Departement de Recherche Fondamentale sur la Matiere Condese, Centre d'Etudes Nucleaires de Grenoble, (France) 1998, Invited Professor: l'Ecole Normale Superieur de Cachan, (France) 2000. Visiting Professor: Tohoku University, Japan, 2002, Member of Polish Chemical Society 1976 - to date, Director of Institute of Coal Chemistry of Polish Academy of Sciences, 2000 – 2005, Visiting Professor: Faculty of Chemistry, Wollongong University Australia 2016, Corresponding Member of Polish Academy of Science - 2021, Member of International Society of Electrochemistry 2005 – to date, member of International Association of Advanced Materials 2019 – to date. More than 260 research papers which received over 12000 citations (H–index of 52). ORCID: 0000–0001–7099–3982.

Cecylia Wardak received the her Ph.D. degree in analytical chemistry in 2004 and her DSc degree in analytical chemistry and electrochemistry in 2015 from Maria Curie Sklodowska University (MCSU), Lublin, Poland. Since then she has been working as associate professor in the Department of Analytical Chemistry of Maria Curie-Sklodowska University. She is an active COST member. Her main scientific interests are research, development, and analytical applications of electrochemical sensors and biosensors. Her latest research focused on the use of nanomaterials and composite materials in the construction of ion-selective electrodes with solid contact. To date, she has published over 100 peer-reviewed scientific papers. ORCID: 0000–0002–5785–3237